Batteryless, Contactless, and Wireless Power Factor and Apparent Power Sensor Using Piezoelectric Film

Short paper

Takaya Yoshitake
Department of Communication Engineering and Informatics
The University of Electro-Communications
Chofu, Japan
Email: y2131168@edu.cc.uec.ac.jp

Shunkichi Takamatsu, Shinichiro Mito
Department of electronic engineering
National Institute of Technology, Tokyo College
Hachioji, Japan
Email: mito@tokyo-ct.ac.jp

Abstract—**Power measurement of individual machines is required in factories for production control and energy conservation. Therefore, a power consumption monitoring sensor that can be easily retrofitted and requires minimal maintenance should be devised. In this study, we developed a contactless, wireless, and battery less alternating current (AC) apparent power and power factor sensor, wherein a current-sensing transformer serves not only as a noncontact current sensor but also as a power supply for the sensor. The AC voltage waveform was measured without a metal contact by using a piezoelectric film. A low-power circuit was designed to manage the power and measure the power factor from current and voltage waveforms. The prototyped sensor was tested in the factory. The data obtained by the field test were consistent with the results obtained from a commercially available power meter. The developed sensor can enable energy savings and carbon dioxide reduction in industrial applications.**

Keywords-electrical power sensing; electric field; noncontact measurement; energy harvesting; SDG.

I. INTRODUCTION

This study expands on a previous conference submission [1]. The reduction of electrical power consumption remains a pertinent issue in factories with regard to reducing manufacturing costs and CO_2 emissions [2][3] so as to ensure compliance with the International Organization for Standardization (ISO) 14001 standard [4]. Therefore, precise measurement of the power consumption of each unit of equipment is critical [5].

Such measurement requires compact, easy-to-install, and inexpensive wireless power sensors. However, existing sensors cannot satisfy these demands [6]–[11].

To measure the current and voltage waveforms without invading the cables, the development of sensors that can be easily retrofitted. Current waveforms can be easily measured using a commercially available split-type current transformer [12]. Current transformers output an induced current that is proportional to the current flowing in the cable to be measured. This current can be used for sensing and power generation for energy harvesting [13]–[16]. Energy-harvesting batteryless operation considerably reduces maintenance costs. However, noninvasive measurement of the voltage waveform is difficult. Several nonmetallic contact methods for voltage waveform

measurement have been proposed [17]–[20] to realize ease of installation and noninvasive measurement. However, these methods are expensive and require multiple probes, which renders implementation difficult.

In this study, we developed a non-metal-contact voltage measurement method based on a single probe using a piezoelectric film. Furthermore, we fabricated and evaluated an energy-harvesting, noninvasive, and retrofittable wireless power consumption sensor that consists of the proposed voltage sensor, a current transformer, an energy-harvesting circuit, a power factor (PF) measurement circuit, and a wireless communication module for use in factories. The device does not require complex electrical circuitry and costs approximately $20 because of its simple design.

In Section 2, a block diagram of the proposed sensor is presented. Section 3 describes the nonmetal contact voltage measurement process using a piezoelectric film. Section 4 presents the power management and PF measurement circuit. Section 5 presents the results of field tests. Finally, Section 6 presents the conclusions of this study.

II. SENSOR CONFIGURATION

The configuration of the developed sensor is illustrated in Figure 1. A current transformer was used to measure the current in a contact-free manner. The operating power of the wireless module can be obtained from the current transformer. The sensor can be powered through energy harvesting. The apparent power was calculated by multiplying the assumed-to-be-constant voltage with the measured current. The PF was calculated using the phase difference between the voltage waveform acquired by the proposed voltage sensor and the current waveform. The obtained apparent power and PF were transmitted using a wireless module (TWE-Lite, Mono Wireless Inc., Kanagawa, Japan).
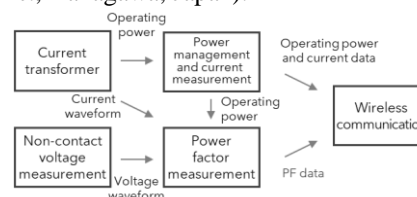

Figure 1. Block diagram of the proposed power factor (PF) and apparent power sensor.

Installation of the developed sensor is easy because noncontact single probes are used for both current and voltage measurements. Furthermore, our sensor requires lower maintenance than conventional sensors because of its energy harvesting-based operation.

III. NON-METAL-CONTACT VOLTAGE MEASUREMENT USING PIEZOELECTRIC FILMS

A. Principle

A piezoelectric film was attached to an electric cable. A cross-sectional view of the cable and piezoelectric film is displayed in Figure 2. The cable was assumed to be a sufficiently long conductor cylinder. When a voltage was applied to the cable, an electric field, E, is generated, and a potential difference is created between the nearby electrode pair of the piezoelectric film. The potential difference $v_p(t)$ can be calculated as follows:

$$v_p(t) = -\int_r^{r+a} E \, dr = \frac{q(t)}{2\pi\varepsilon_0\varepsilon_r}\ln\frac{r+a}{r} \qquad (1)$$

In Equation (1), r is a distance between the center of the cable to a nearest electrode, a is a thickness of the dielectric film, and $q(t)$ is the charge per unit length of the cable.

Energized cables and grounded cables have capacitance. Therefore, the voltage applied to cable $v(t)$ and the charge per unit length of cable $q(t)$ have the following relationship:

$$q(t) = Cv(t) \qquad (2)$$

where C is the capacitance formed between the cables, which is extremely small. Combining the two equations, the relationship between the potential difference $v_p(t)$ and cable voltage $v(t)$ can be expressed as follows:

$$v_p(t) = \frac{Cv(t)}{2\pi\varepsilon_0\varepsilon_r}\ln\frac{r+a}{r} \qquad (3)$$
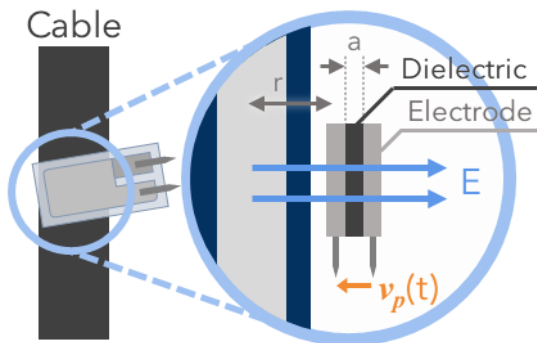

Figure 2. Cross-sectional view of the cable and piezoelectric film

If the piezoelectric film is placed near the cable and r is small, the output voltage $v_p(t)$ has a sufficient value for measurement, and it correlates with cable voltage $v(t)$. Therefore, the voltage can be measured without a metal contact. Equation (3) indicates that the output voltage $v_p(t)$ is proportional to the thickness of the piezoelectric film.

However, the output of the piezoelectric film depends on the distance.

B. Prototyping

Noninvasive voltage measurement can be realized using by measuring the electric field strength around a wire using a single probe when the voltage is applied to the wire [17][18]. We used piezoelectric films to realize a low-cost electric field measurement method. Piezoelectric films comprise a piezoelectric material sandwiched between metal electrodes. The piezoelectric material was polarized by the electric field around the wire, and a potential difference was generated between the two electrodes. Thus, the electric field around the wire could be detected using a single piezoelectric probe.

A non-metal-contact voltage probe was prototyped, as displayed in Figure 3. A commercially available piezoelectric film (LDT0-028K, TE Connectivity, Schaffhausen, Switzerland) was bent and placed at a uniform distance from the center of the wire. The sensor frame was fabricated using a 3D printer (UP BOX Plus, Beijing Tiertime Technology Co. Ltd., Beijing, China). The cable-side electrode was set as positive.
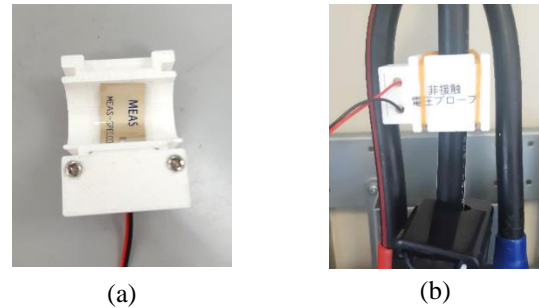

(a)   (b)

Figure 3. (a) Fabricated non-metal-contact voltage probe. (b) Probe placed on the electric cable.

C. Measurement

The voltage waveform observed using the probe is displayed in Figure 4. Although the output voltage and phase varied with the distance between the piezoelectric film and the wire, the correlation coefficient obtained for the actual and measured waveforms was 0.99. The proposed method can measure the relative change in the voltage, which is sufficient to enable PF calculation. The piezoelectric sensor output was related to the actual voltage and was consistent with the calculation results from the equivalent circuit. Furthermore, the output was almost zero when the neutral side of the cable was measured, which indicated that hum noise was not measured.
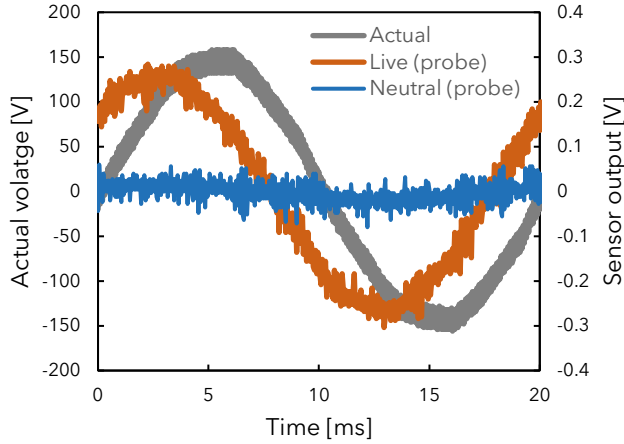
Figure 4. Results of non-metal-contact voltage measurements using the piezoelectric film. The piezoelectric sensor output was related in advance to the actual voltage. The neutral side output is almost zero.

D. Linearity of the output for the applied electric field

To evaluate the probe characteristics against the voltage applied to the cable, we measured the relationship between the applied electric field strength and output. A conductive tape was attached to both sides of the piezoelectric film, and a signal generator was used to apply voltage to the tape. The results displayed in Figure 6 confirmed that the output was linear with respect to the applied electric field. The inclination was slightly larger at higher frequencies.
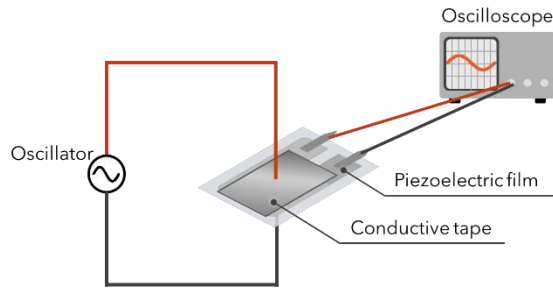

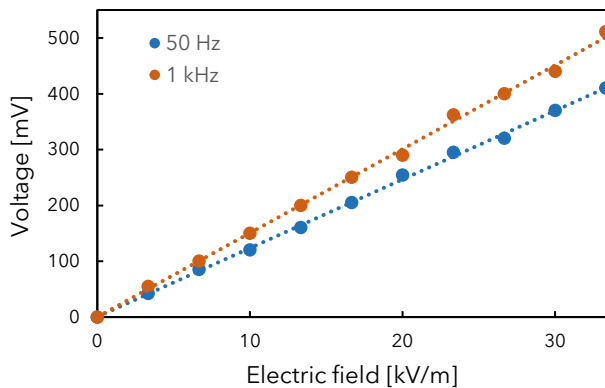Figure 5. Evaluation of the probe characteristics for the applied electric field.

Figure 6. Output voltage of the probe for electric field intensity. Output has linearity to the applied electric field.

E. Frequency response

The frequency response of the output of the fabricated probe was measured. The voltage of the measured cable was 100 V_{rms} for all frequencies. The obtained frequency characteristics are displayed in Figure 8. The gain reference was set to the output at 350 Hz. The cutoff frequency was 25 Hz, which indicated excellent low-frequency characteristics.
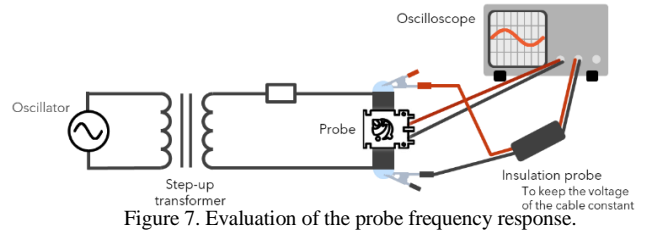

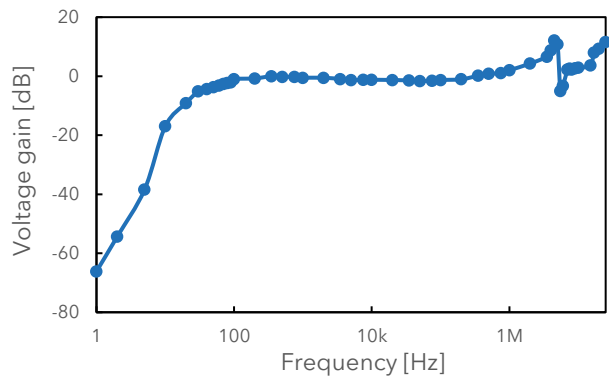Figure 7. Evaluation of the probe frequency response.

Figure 8. Frequency response of the voltage measurement by the piezoelectric film. The gain reference was set to the output at 350 Hz. The sensor gain was stable in the range of 80 Hz to 1 MHz and the cutoff frequency was 25 Hz.

IV. CIRCUIT OF THE PROPOSED METHOD

A. Power management and current measurement circuit

The power management circuit of the fabricated sensor is illustrated in Figure 9. A current transformer was installed on the cable to be measured, and the current obtained from the transformer was full-wave rectified, smoothed, and measured. The power management circuit outputted not only the operation power for the entire circuit but also the voltage that correlated with the current flowing in the cable.
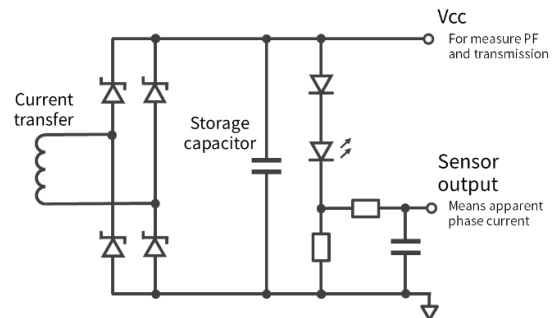

Figure 9. Overview of the power management circuit.

First, we simulated the transient response of the power supply voltage (V_{cc}) of the power management circuit when currents of 1, 5, 10, 20, and 30 A were applied to the measured cable. The circuit used in the simulation is illustrated in Figure 10. Here, C_1, L_1, and R_1 on the primary side of the transformer are the equivalent circuits of the cable. The simulation results for V_{cc} are displayed in Figure 11, which reveals V_{cc} converges after a few seconds. Furthermore, the results revealed that the voltage depended on the amount of current flowing through the cable. Here, V_{cc} was determined by a measurement resistor R_6 (47 Ω) and D_5 and D_6. We confirmed that the operating voltage of a general micro controller (1.8 to 3.6 V) can be obtained in the range 1 to 20 A, where we want to perform the measurement. The measurement range of the current can be modified by changing the resistance value or the threshold of the diodes.
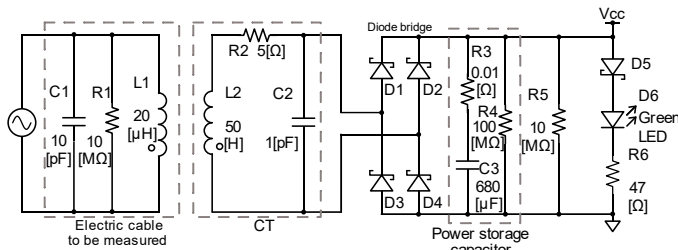

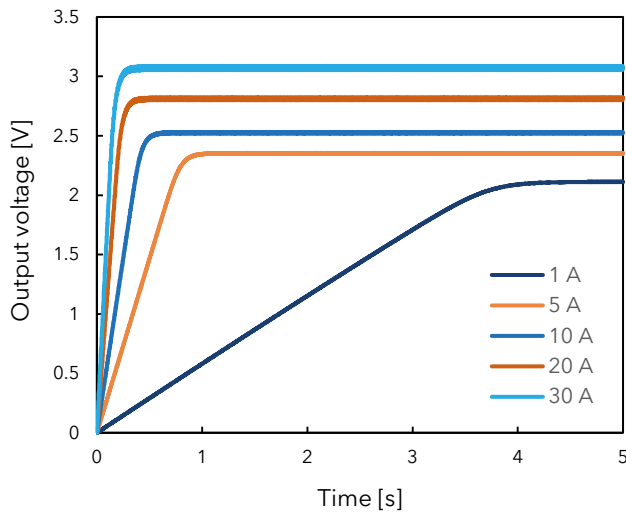Figure 10. Simulation circuit for the cable current and supply voltage for the sensor.

Figure 11. Simulation results of the cable current dependence on the supply voltage (V_{cc}). V_{cc} converges after a few seconds and depends on the amount of current flowing in the cable.

Next, we simulated the relationship between the measured current and the sensor output voltage. The current transformer was assumed to be a current source that outputs current proportional to the current flowing in the cable. The circuit displayed in Figure 12 was simulated.
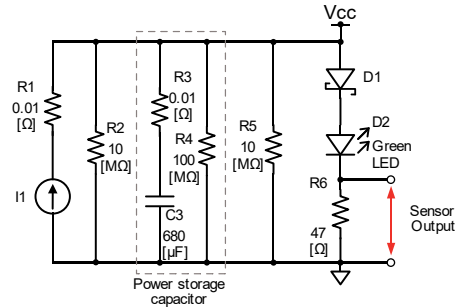

Figure 12. Simulation circuit of the power management circuit with the input current.

The results of the relationship between the current, power supply voltage for our sensor, and the voltage of R_6 are displayed in Figure 13. The supply voltage was rapidly increased to the operating voltage of the microcontroller. However, the sensor output was proportional to the output of the current transformer. The power management circuit simultaneously generated both the power supply and current measurement voltages.
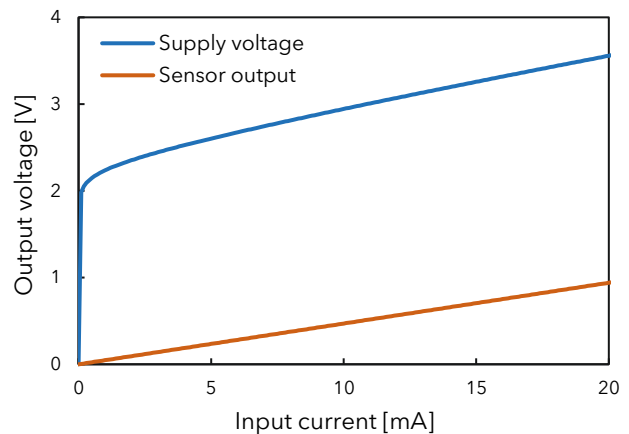

Figure 13. Simulation results of the sensor supply voltage and the sensor output for the input current. The supply voltage rapidly increases to the operation voltage of the micro controller. By contrast, the sensor output is proportional to the output of the current transformer

The sensor output was changed by the power consumption of the microcontroller. The microcontroller sent the data every 5 s and consumed 15 mA for 4 ms to send the data. For the other 4996 ms, the microcontroller was in the sleep mode and consumed 1.5 µA. An RC low-pass filter with a time constant of 1 s was used to reduce the influence of the sending current.

B. PF measurement circuit

The developed sensor was operated using the power obtained from the current transformer; thus, realization of low-power PF measurement was critical. In this study, we used an analog circuit to perform PF measurements with a low power consumption.
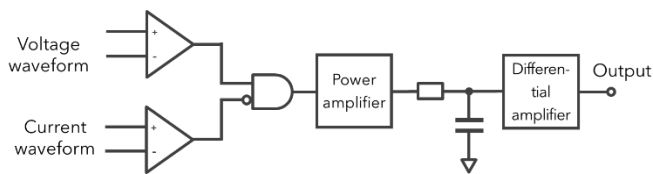
Figure 14. Block diagram of the PF measurement circuit.

Figure 14 displays the block diagram of the fabricated PF measurement circuit. The current and voltage waveforms were converted into square waves, and the phase difference was obtained as the pulse width by calculating the logical product of these waves. Subsequently, the phase difference was output as an analog voltage through the power amplification, smoothing, and differential amplification processes. The output was connected to the analog-to-digital converter of the wireless module, and the data were transmitted. This circuit can be applied to both the single- and three-phase electrical loads.

V. FABRICATION AND FIELD TEST

Noncontact wireless apparent power and PF sensors were fabricated, as displayed in Figure 15. The fabricated sensor was attached to an injection molding machine (SH100C, Sumitomo Heavy Industries, Tokyo, Japan) for field testing (Figure 16).
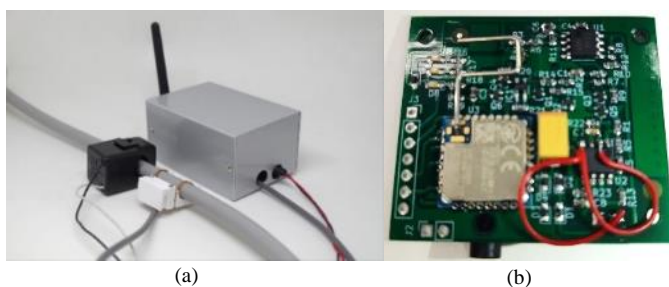

Figure 15. (a) Fabricated sensor. The black probe is the current transformer, and the white probe is the voltage probe developed in this work. The silver box contains the processing circuit. (b) Fabricated sensor board.

Figure 16. Overview of the field test. The fabricated probes and circuit were applied to the injection molding machine.
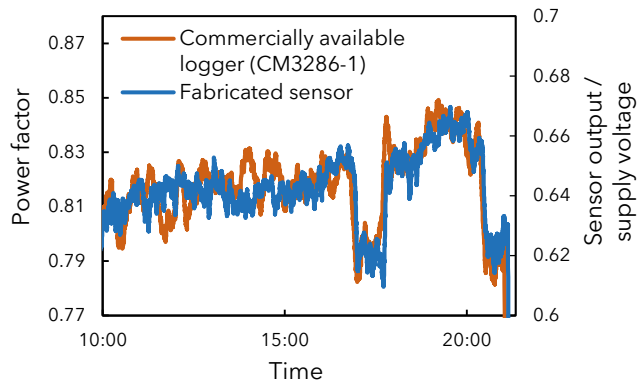

Figure 17. Comparison of the PFs obtained from a commercially available logger and the fabricated sensor.
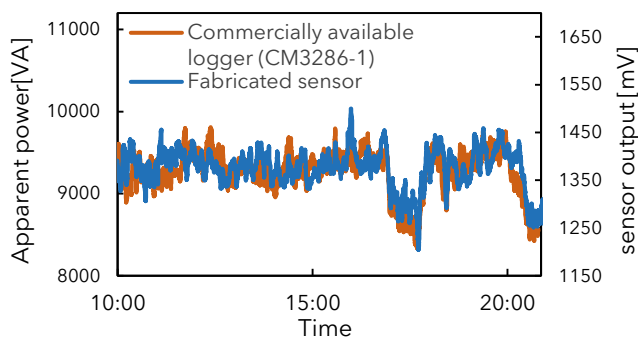

Figure 18. Comparison of the apparent power results obtained from a commercially available logger and the fabricated sensor.

Figures 17 and 18 display comparisons of the PFs and apparent power values, respectively, which were measured using the developed sensor with those measured using a commercially available power logger (CM3286-01, HIOKI E.E., Tokyo, Japan). The PF obtained by the developed sensor had a correlation coefficient of 0.80 with that measured using a commercial logger. Apparent power had a correlation coefficient of 0.73. These results indicate that the proposed sensor can measure the power consumption sufficiently accurately. This accuracy is suitable for rough logging of the PF and can be improved by calibration and grounding processes.

VI. CONCLUSION

Voltage waveforms were measured using a single piezoelectric probe without metal contacts. Novel energy-harvesting wireless apparent power and PF sensors were developed using the piezoelectric probe. The data acquired using the developed sensor were consistent with the data acquired using a commercially available power meter.

REFERENCES

[1] T. Yoshitake, S. Takamatsu, and S. Mito, "Development and application of an energy harvesting power factor and apparent power sensor" in SENSORCOMM 2021, Athens, Greece, Nov. 2021, pp. 8-10, Accessed: 2022.05.10 [Online]. Available from: https://www.thinkmind.org/index.php?view=article&articleid=sensorcomm_2021_1_20_10010

[2] A. Hawkes, "Estimating marginal CO2 emissions rates for national electricity systems," Energy Policy, vol. 38, pp. 5977-5987, 2010.

[3] T. Unger and E. O. Ahlgren, "Impacts of a common green certificate market on electricity and CO2-emission markets in the Nordic countries," Energy Policy, vol. 33, pp. 2152-2163, 2005.

[4] P. Gupta, "End of life considerations for EV batteries - ISO and Indian business perspectives," 6th Hybrid and Electric Vehicles Conference (HEVC 2016), 2016, pp. 1-5, doi: 10.1049/cp.2016.0989.

[5] W. Gans, A. Alberini, and A. Longo, "Smart meter devices and the effect of feedback on residential electricityconsumption: Evidence from a natural experiment in Northern Ireland," Energy Economics, vol. 36, pp. 729-743, 2013.

[6] B. K. Barman, S. N. Yadav, S. Kumar, and S. Gope, "IOT Based Smart Energy Meter for Efficient Energy Utilization in Smart Grid," 2018 2nd International Conference on Power, Energy and Environment: Towards Smart Technology (ICEPE), 2018, pp. 1-5, doi: 10.1109/EPETSG.2018.8658501.

[7] T. Sirojan, S. Lu, B. T. Phung, and E. Ambikairajah, "Embedded Edge Computing for Real-time Smart Meter Data Analytics," 2019 International Conference on Smart Energy Systems and Technologies (SEST), 2019, pp. 1-5, doi: 10.1109/SEST.2019.8849012.

[8] P. Kumar and U. C. Pati, "IoT based monitoring and control of appliances for smart home," 2016 IEEE International Conference on Recent Trends in Electronics, Information & Communication Technology (RTEICT), 2016, pp. 1145-1150, doi: 10.1109/RTEICT.2016.7808011.

[9] A. S. Musleh, M. Debouza, and M. Farook, "Design and implementation of smart plug: An Internet of Things (IoT) approach," 2017 International Conference on Electrical and Computing Technologies and Applications (ICECTA), 2017, pp. 1-4, doi: 10.1109/ICECTA.2017.8252033.

[10] W. Hlaing et al., "Implementation of WiFi-based single phase smart meter for Internet of Things (IoT)," 2017 International Electrical Engineering Congress (iEECON), 2017, pp. 1-4, doi: 10.1109/IEECON.2017.8075793.

[11] C. Huang, T. Hsien, and G. Jong, "Indoor power meter combined wireless sensor network for smart grid application," 2012 8th International Conference on Information Science and Digital Content Technology (ICIDT2012), 2012, pp. 336-339.

[12] V. Miron-Alexe, "Comparative study regarding measurements of different AC current sensors," 2016 International Symposium on Fundamentals of Electrical Engineering (ISFEE), 2016, pp. 1-6, doi: 10.1109/ISFEE.2016.7803152.

[13] T. L. Companhoni, M. Götz, C. Protasio, and I. Müller, "Development of a Wireless Current Measurement Sensor Node for IoT Applications," 2018 VIII Brazilian Symposium on Computing Systems Engineering (SBESC), 2018, pp. 1-7, doi: 10.1109/SBESC.2018.00010.

[14] T. -C. Huang et al., "120% Harvesting Energy Improvement by Maximum Power Extracting Control for High Sustainability Magnetic Power Monitoring and Harvesting System," in IEEE Transactions on Power Electronics, vol. 30, no. 4, pp. 2262-2274, April 2015, doi: 10.1109/TPEL.2014.2330868.

[15] V. Pavel, Ž. Jiří, K. Jindřich, K. Kamil, S. Jiří, and G. Vjačeslav, "Energy Harvesting and Communication Systems for Power Lines Inspection Robot," 2020 21st International Scientific Conference on Electric Power Engineering (EPE), 2020, pp. 1-4, doi: 10.1109/EPE51172.2020.9269193.

[16] P. Kamat, D. Sutar, and P. Pavan Prasad, "Efficient Energy Harvesting Using Current Tranformer for Smart Grid Application," 2018 2nd International Conference on Trends in Electronics and Informatics (ICOEI), 2018, pp. 343-347, doi: 10.1109/ICOEI.2018.8553892.

[17] D. Onishi et al., "Surface potential measurement of stress grading system of high voltage rotating machine coils using pockels field sensor," 2017 International Symposium on Electrical Insulating Materials (ISEIM), 2017, pp. 95-98, doi: 10.23919/ISEIM.2017.8088697.

[18] C. Peng, P. Yang, X. Wen, D. Fang, and S. Xia, "Design of a novel micromachined non-contact resonant voltage sensor for power distribution systems," SENSORS, 2014 IEEE, 2014, pp. 978-981, doi: 10.1109/ICSENS.2014.6985166.

[19] A. Rodriguez-Garde, A. B. Socorro-Leranoz, M. E. Martinez, J. Goicoechea, and I. R. Matias, "Dynamic Response of Gold-coated Optical Fiber Sensors Subjected to Voltage Variations," 2020 IEEE SENSORS, 2020, pp. 1-4, doi: 10.1109/SENSORS47125.2020.9278838.

[20] P. S. Shenil, R. Arjun, and B. George, "Feasibility study of a non-contact AC voltage measurement system," 2015 IEEE International Instrumentation and Measurement Technology Conference (I2MTC) Proceedings, 2015, pp. 399-404, doi: 10.1109/I2MTC.2015.7151301.